03,07,09

High-temperature diffusion of beryllium in AlN as an area to solve problem of *p*-type doping and reduce intensity of optical absorption

© E.N. Mokhov, S.S. Nagalyuk, O.P. Kazarova, V.A. Soltamov

Ioffe Institute,
St. Petersburg, Russia

E-mail: Mokhov@mail.ioffe.ru

Received May 25, 2025
Revised May 25, 2025
Accepted May 27, 2025

Single-crystal aluminum nitride (AlN) is a promising material for development of ultraviolet optoelectronic and power instruments due to a wide band gap ($E_g \approx 6.1$ eV). The design of the instrument fleet on its basis is restricted by difficulties in implementation of *p*-type doping, to a large extent due to poor knowledge of acceptor impurity properties. Traditionally used magnesium (Mg) impurity in AlN is characterized by high energy of activation and low solubility. The review considers the studies on AlN doping with beryllium (Be) — impurity with low energy of activation (~ 37 meV), high solubility and atomic radius close to Al. Special attention is paid to method of high-temperature diffusion of Be into single-crystal AlN, which demonstrated efficiency of Be as an acceptor. It was also shown that Be decreases the coefficient of optical absorption of AlN in a wide spectrum. The obtained data opens the path to development of *p*−*n*-structures based on AlN and design of optical instruments of ultraviolet range.

Keywords: aluminum nitride of *p*-type, beryllium diffusion, absorption spectrum.

DOI: 10.61011/PSS.2025.06.61684.141-25

1. Introduction

Semiconductors of III-nitride family (InN, GaN, AlN) and their solid solutions ($Al_xGa_{1-x}N$, InGaN) are the key materials of modern optoelectronics, power and high-frequency electronics [1,2]. One of the prominent representatives of this family is aluminum nitride (AlN), having an extremely wide direct structure ($E_g \approx 6.1$ eV) [1]. Thanks to this, AlN is used in development of sources of ultraviolet radiation (UV-B, UV-C) and high-voltage and high-frequency instruments [1,2].

It should be noted that same as in the case of gallium nitride, the successful introduction of AlN into semiconductor electronics requires the solution to two key tasks. Firstly, it is necessary to master the technology to produce volume single-crystal substrates with diameter of 2 in min., which is the minimum industrial standard. Secondly, it is required to develop a reproducible method of crystal synthesis with *p*-type of conductivity. Currently the first of the identified tasks is being successfully solved by active development of technology to grown volume AIN crystals technology with diameter of 2 and 4 in by method of physical vapor transport (PVT) [3–6]. The second task is also delicate and requires fundamental approach. Same as in the case of GaN, AlN demonstrates susceptibility to electron type of conductivity, provided for by uncontrolled doping with donor impurities, such as silicon in the position of Al(Si_{Al}) substitution and oxygen that substitutes nitrogen (O_N). The task of effective introduction of acceptor impurities with low energy of activation (E_a) into AlN remains relevant. The situation reminds an early stage of GaN research, when *p*-type of conductivity was achieved only after development of effective methods for activation of acceptor Mg impurity. In particular, use of low-energy electron-beam irradiation (LEEBI) [7] and high-temperature annealing [8] made it possible to obtain GaN with reproducible *p*-type of conductivity, which became a key factor in development of GaN-based instruments. Similarly, the search for and implementation of effective methods of *p*-type doping in AlN is a critical task, without solution to which it is not possible to create full-scale electronic and optoelectronic devices based on this material. In case of AlN it is known that E_a of magnesium depends on the content of aluminum in solution $Al_xGa_{1-x}N$. Namely, $E_a(Mg_{Al})$ increases practically linearly as the Al concentration grows in the solution, and when the value is $x > 0.6$, Mg stops giving a noticeable acceptor contribution, being characterized by E_a of around 400 meV [9] and achieving $0.5-0.6$ eV in case of pure aluminum nitride ($x = 1$) [10]. In virtue of such substantial value of activation energy and concurrently relatively low solubility of Mg in AlN, also negatively affecting the concentration of free carriers, the attempts were made to introduce alternative doping impurities, such as beryllium and zinc [11–13].

Investigations of electrophysical properties of beryllium-doped AlN during growth by metalorganic molecular-beam epitaxy (MME) method have identified unique properties of Be as an acceptor impurity. In particular, these experiments confirmed the acceptor type of conductivity in these crystals, and also found that E_a(BeAl) made around 37 meV [11], which is more than ten times lower than E_a(MgAl). In combination with high solubility of Be in AlN

it made it possible to obtain high concentrations of holes, of around $10^{18}\,cm^{-3}$, at room temperature. These results made it possible to create effective homogeneous $p-n$-transitions on AlN, which is a significant achievement in the development of photonics and high-frequency electronics in trinitrides [14]. The important feature of Be impurity in AlN is the proximity of atomic radius of Be, 1.12 Å, to radius of Al atom it substitutes (1.18 Å). This is exactly the fact that sets apart the substituting Be impurity from Mg, having radius of 1.45 Å, which causes reduction in solubility of Mg in AlN and increase of acceptor level activation energy. This circumstance is reflected well in the literature on the study of Mg in GaN, for which the situation is the opposite: size of Ga atom (1.36 Å) is close to size of Mg, making it possible to use the latter for effective doping of *p*-type. The studies of Be behavior in GaN both by experimental and theoretical methods only confirm this trend [15–17].

In virtue of the above, we see it fit to provide the review of the results that our team obtained from the study of properties in AlN doped with beryllium impurity. Namely, we proposed the alternative method of single-crystal AlN doping with beryllium by high-temperature ($T_d = 1700-1800\,^\circ C$) diffusion [12]. It was established that in process of such diffusion Be mostly behaves as an acceptor impurity that compensates donor centers. We also demonstrated that Be has high diffusion constant $D = 10^{-7}-10^{-6}\,cm^2/s$ in AlN, and its introduction causes reduction of optical absorption (OA) of the latter both in the visible and ultraviolet ranges [18]. Production of Be-doped crystals was shown, which were characterized with OA coefficient $\alpha < 30\,cm^{-1}$ in the spectral range 240–700 nm, which is at the level of best specimens of single-crystal AlN [19]. The above results were obtained in process of AlN : Be research by methods of laser-induced breakdown spectroscopy (LIBS), electron paramagnetic resonance (EPR), luminescent microscopy, optical absorption spectroscopy and Raman scattering (Raman scattering spectroscopy).

2. Experimental part

Single-crystal volume specimens of AlN were studied, which were grown by PVT method [3]. For Be diffusion into specimens of single-crystal AlN, plates were cut from the grown ingots with thickness from 0.3 to 1.5 mm, which were further ground and polished. The diffusion process was carried out from tantalum carbide in nitrogen atmosphere in a closed vessel. High purity metallic Be was used as a diffusant that was placed in a boron nitride crucible. The test specimens were placed on a BN plate in an area with the minimum temperature gradient. Diffusion temperature varied from 1700 to 2100 °C, the annealing duration was 0.5–10 h. Note that for the time of diffusion annealing, specimens evaporation was negligibly low due to high temperature resistance of AlN.

In order to determine the impact of purely temperature properties at AlN properties, prior to Be diffusion the studied specimens were annealed under the same conditions. The studies of the annealed crystals found no changes in the color, optical absorption or spectral characteristics of EPR signals compared to the specimens prior to annealing. AlN studies using the method of photoluminescent microscopy were carried out on a microscope MLD-1 with fixation of intensity and color of luminescence excited by the ultraviolet source of light. LIBS spectra, which unambiguously indicate the presence of Be impurity in AlN after the diffusion process, were recorde by a high-speed receiver-spectrometer AvaSpec-ULS2048LUSB2, operating in a spectral range 336–886 nm with spectral resolution 1 nm. To excite the spark plasma, pulse laser Nd^{3+} : YAG LQ-129, SolarLC JSC was used. Repetition rate of laser pulses 2 Hz, pulse duration 28 ns, energy 85 mJ. Optical absorption spectra of initial AlN crystals, after high-temperature annealing and after the diffusion process, were recorded on a spectrometer Shimadzu-2450 UV/Vis at room temperature. Micro-Raman spectra were recorded at room temperature using Horiba Jobin Yvon T64000 spectrometer equipped with confocal microscope. To excite the spectra, Nd : YAG-laser was used ($\lambda = 532$ nm, $E = 2.33$ eV). Studies with EPR method were carried out using a spectrometer of X-range (~ 9.3 GHz) Bruker Elexsys E600 in the continuous mode.

3. Results and discussion

As noted in the introduction, AlN doping with Be impurity in process of high-temperature diffusion causes considerable change in the optical characteristics of crystals. This result is illustrated in Figure 1, which provides the photographs of two AlN specimens cut from two different single-crystal AlN plates.

The spectral confirmation of the fact that high-temperature annealing of AlN in Be vapors causes introduction of the latter into a crystal was obtained by us from the LIBS experiment results shown in Figure 2, *a*. You can see that apart from the common uncontrolled impurities in AlN, such as carbon, oxygen and silicon, additional spectral lines appear in the plasma glow from the specimens after diffusion on wavelengths $\lambda = 456.9-466.1$ nm. These plasma radiation lines agree well with the spectral lines of neutral beryllium Be(I) and once ionized beryllium Be(II) (Figure 2, *b*), with tabulated values of wavelengths 457.3 and 467.3 nm accordingly [20]. This observation unambiguously confirms the successful doping of AlN with beryllium using method of high-temperature diffusion.

It should be noted that the small value of ion radius Be^{2+}, $r = 0.45$ Å, makes it possible to introduce impurity to the considerable depth of the specimen, down to 1700 μm, according to the results of luminescence recorded from the ends of the AlN specimens before and after diffusion (Figure 2, *c*). Therefore, in specimen *2* you can see the near-surface layer with thickness of 100 μm with bright

green luminescence, and in the specimen *3* with thickness 1700 μm the glow is observed in the entire thickness of the specimen, and at the same time you can see the near-surface layer with thickness of 80 μm having a prominent effect of luminescence quenching. The availability of data on the thickness of the diffusion layer and temperature mode made it possible to assess the beryllium diffusion constant, using the formula to describe diffusion from a constant source:

$$N(x,t) = N_0 \operatorname{erfc}\{x/[2(Dt)^{1/2}]\}, \qquad (1)$$

where N_0 — surface concentration, $N(x,t)$ — concentration of diffusing impurity depending on the depth and time, D — diffusion constant, x — diffusion depth, t — diffusion time [21]. As a result of the completed assessment it was found that at the ratio of concentrations $N(x,t)/N_0 = 10^{-2}$ the diffusion constant of beryllium is 10^{-7} cm^2/s [16]. Besides, it should be noted that the concentration quenching of luminescence observed in the specimen doped with Be at 2100 °C, is usually observed at concentration of doping impurities $n \geq 10^{19}$ cm^{-3}, which indicates high concentrations of Be impurities obtained as a result of diffusion doping.

Despite the significant temperatures of the diffusion process and high concentrations of introduced impurities, the crystalline perfection of AlN undergoes no noticeable deteriorations, which follows from Raman spectra recorded in the specimens before and after diffusion, given in Figure 3. For more detailed analysis, the specimen *2* was

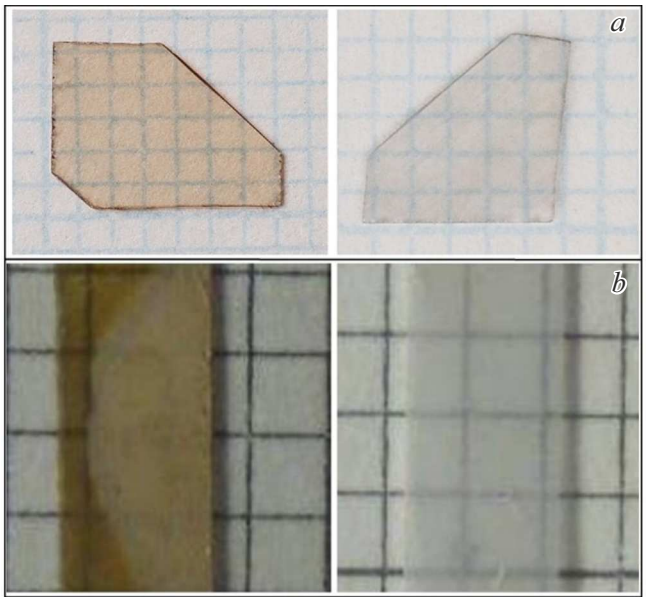

Figure 1. The right column shows a typical view of AlN crystals prior to diffusion; a prominent amber-yellow color is seen. Typical AlN specimens doped with Be as a result of diffusion at temperature 1800 °C are shown on the left. You can see that AlN : Be crystals are transparent, and the presence of Be in the crystal causes visual disappearance of optical absorption in the visible range.

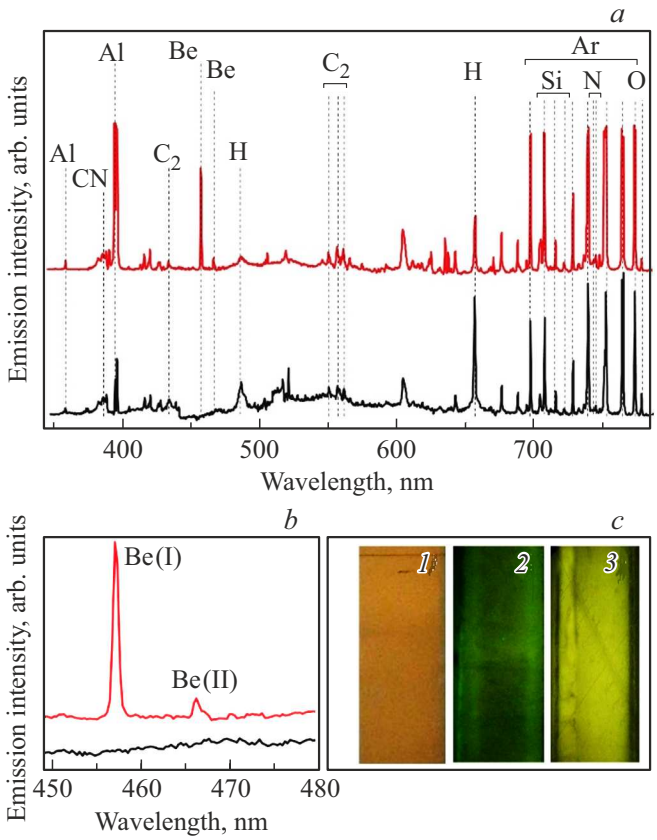

Figure 2. *a*) LIBS-spectra of AlN specimen. The lower spectrum is recorded in an AlN specimen prior to Be diffusion, the upper spectrum — in the same specimen after Be diffusion. The dashed lines show the positions of plasma emission of the corresponding chemical elements. *b*) Spectral lines of beryllium with maximum of intensities in the wavelength range $\lambda = 455-470$ nm, indicated as Be(I) and Be(II), are shown on an enlarged scale. *c*) Luminescence at 300 K for AlN specimen ends: *1* — prior to diffusion; *2* — after Be diffusion 1860 °C, 2 h; *3* — after Be diffusion 2100 °C, 2 h. In *2* you can see brighter layers at the edges of the crystal, in the specimen *3* you can see a dark near-surface layer with thickness of 80 μm.

studied using micro-Raman scattering spectroscopy in the scattering configuration $z(x,x)\overline{z}$. Frequencies of observed modes $A_1(LO)$ and E_2 amounted to 890 and 657.4 cm^{-1} accordingly, which agrees well with the known values for high-quality single crystals of AlN [22]. According to the literature data, the frequency shift of mode E_2 is sensitive to residual mechanical stresses, and its half-width reflects the defect level in the crystalline lattice [23]. As you can see from the insert in Figure 3, the halfwidth of mode signal E_2 before and after diffusion is within 3.4–3.6 cm^{-1}, which is comparable to the specific value 3 cm^{-1} for AlN single crystals of high crystalline quality [24]. Therefore, you may conclude that beryllium diffusion at high temperature has no significant effect on the structural quality of the material.

Besides, the considerable clarification of AlN specimens from Be doping is observed, as seen in Figure 4, *a* and *b*.

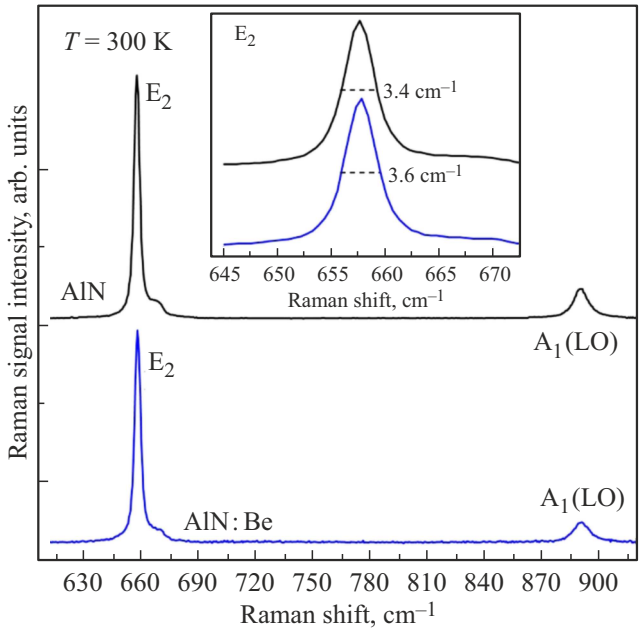

Figure 3. Raman scattering spectra (Raman-spectra) of AlN wurtzite structure, recorded at room temperature on the surface (0001). The upper spectrum is obtained from the initial AlN crystal, the lower one — after Be diffusion. The insert highlights a section of Raman scattering spectrum with spectrum E_2.

In particular, the wide band of optical absorption with maximum at the wavelength 450 nm, responsible for amber-yellow color of initial crystals, disappears, and the absorption in the UV-area of the spectrum decreases significantly, 220–320 nm. Based on the literature data available today, the absorption band in the blue area of the specimen, the spectrum of which is given in Figure 4, *a*, arises due to the presence of nitrogen vacancies in the crystal in the neutral charge state (V_N^0) or complex defects related to V_N^0-centers [25–27]. Absorption in the deep UV-area is explained by three different models. Thus, in article [28] this absorption is explained by transition of electron from a deep acceptor — a negatively charged carbon, substituting nitrogen atom (C_N^-) — into the conduction band. Thermodynamic level of transition $(0/-)$ of this defect arises, when Fermi level (E_F) is 2 eV higher than the valence band limit energy (E_V). Therefore, the absorption at wavelength 265 nm, related to transition $C_N^- \rightarrow C_N^0 + \overline{e}$, is stable at any position E_F in the band gap is higher than $E_V + 2$ eV. On the contrary, if E_F is below this level, the absorption is suppressed. The latter agrees with our experimental data obtained before and after beryllium diffusion. Indeed, nominally non-doped AlN is a high-resistance material of *n*-type, so that E_F is located in the upper half of the band gap, which causes the appearance of optical absorption (OA) at 265 nm. If you assume that beryllium introduced in AlN by diffusion acts mainly as an acceptor, you should expect displacement of E_F towards the valence band top. Such displacement makes negative charge state C_N^- unstable and, as a result, causes absorption quenching, as you can see from spectra (3) in Figure 4, *a* and *b*. Substantial displacement of Fermi level is possible, since the activation energy of beryllium acceptors was previously assessed at around 37 meV [11]. Different OA bands in AlN were studied in paper [27] using hybrid functional estimates. It is shown that the aluminum vacancies and complexes with oxygen cause appearance of absorption bands with the maximum at 4.0 eV (310 nm) and above. Optical absorption by these complexes is related to thermodynamic levels of transitions $(2-/-)$ and $(-/0)$, which are stable at E_F higher than $E_V + 2.59$ eV. Therefore, OA is suppressed when E_F is displaced below this level. Such displacement may be provided, if you assume that after diffusion the Be impurities mostly form acceptor type centers. In paper [29] based on IR spectroscopy data it was shown that negatively charged state of tricarbon defect $(C_N{-}C_{Al\text{-}C}{-}C_N)$ contributed greatly to the absorption band at 265 nm, which corresponds to optical transition of electron from the lower level $(-/0)$ of this defect to the conduction band, which is possible at E_F in the middle of

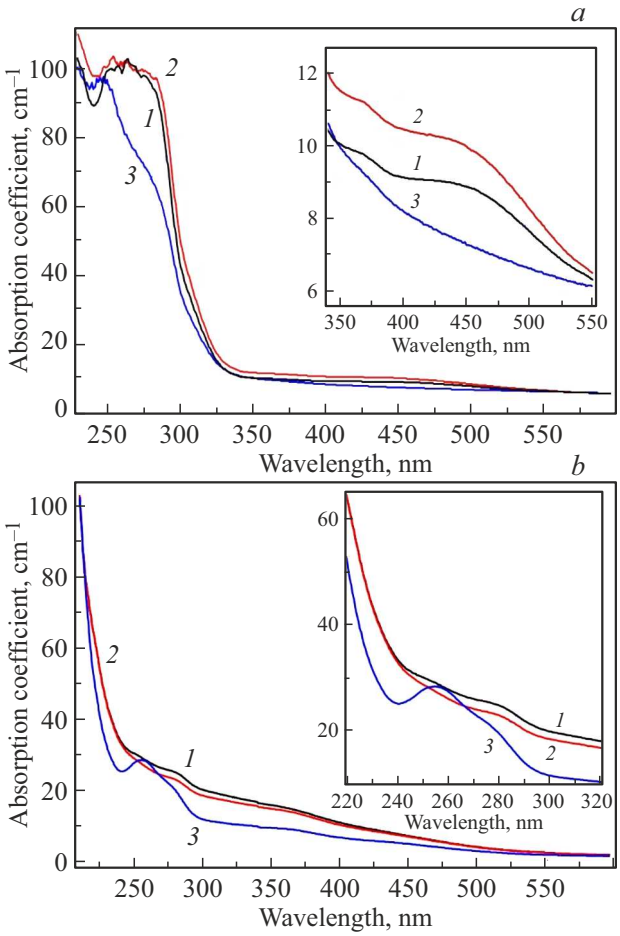

Figure 4. Absorption coefficient in *a*) visible and *b*) ultraviolet ranges: *1* — for initial AlN specimens, *2* — for specimens after annealing, *3* — for specimens after annealing and diffusion of Be. The inserts show spectral ranges 350–550 and 220–320 nm.

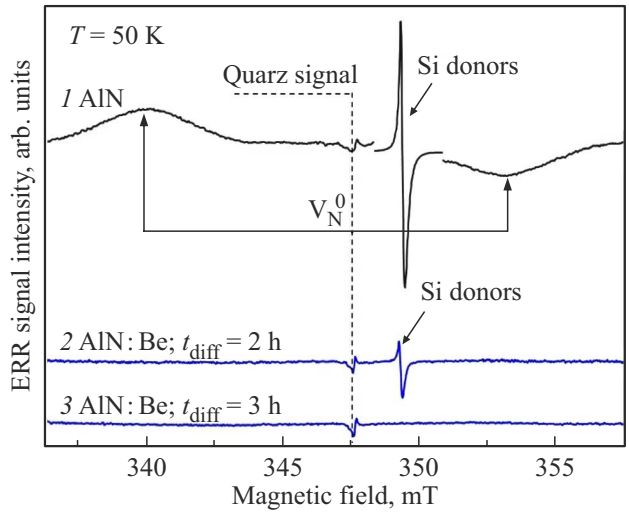

Figure 5. EPR spectra of AlN specimen before (*1*) and after (*2, 3*) beryllium diffusion, measured at $T = 50\,\mathrm{K}$ under excitation with laser radiation having wavelength $\lambda = 403\,\mathrm{nm}$. The comparison signal, corresponding to the quartz tube where the specimen is inserted, is indicated with a dashed line. The EPR signal from small silicon donors is shown with the amplitude on the spectrum reduced 10 times *1*. EPR signals from a nitrogen vacancy in the neutral charge state V_N^0 are shown with arrows

the band gap. Absorption is suppressed, when E_F is below level $(-/0)$, which corresponds to the impact of acceptor impurity of Be at position of E_F.

After the consideration of the impact from defects and their charge states to the optical absorption of AlN and impact of Be impurity at the Fermi level position, it is necessary to show that the presence of Be impurity in the crystal really shifts the Fermi level towards the valence band limit, and changes the charge state of impurities and defects. For this purpose we did experiments on electron paramagnetic resonance in AlN crystals before and after Be diffusion. The corresponding spectra are shown in Figure 5. You can see that before Be diffusion, AlN specimen contained two types of paramagnetic centers, previously identified as V_N^0 [30] and as impurity of substitution of aluminum atoms with silicon (Si_{Al}), forming small donors [30,31]. Besides, the EPR signal Si_{Al} is characterized with high amplitude and is shown in the figure as having diminished 10 times relative to the signal from the quartz tube, the amplitude of which does not depend on the studied specimen. The EPR $(2, 3)$ spectra recorded in the specimens after Be diffusion under the same conditions as the spectrum (1) have an interesting feature. Namely, in the specimen after the diffusion process with duration of 2 h the EPR signals from V_N^0-centers were not observed, and amplitude of the signal from small donors Si_{Al} decreased significantly. Longer process of diffusion for 3 h made it possible to finally suppress the EPR signal of donors, as you can see from the spectrum (3). Both of these observations indicate the compensation of paramagnetic centers of donor type due to introduction of Be into AlN, which means the shift of Fermi level position to the lower half of the AlN band gap. It should be noted separately that disappearance of EPR spectra from V_N^0-centers correlates well with the disappearance of the absorption band at wavelength 450 nm, as it is observed in OA spectra given in Figure 4. Therefore, EPR-spectroscopy unambiguously demonstrated that Be introduced in AlN by method of high-temperature diffusion, has acceptor nature and clarifies AlN single crystals.

4. Conclusion

An alternative approach was demonstrated to doping of single-crystal AlN with beryllium, based on its high-temperature diffusion at 1700–1800 °C. The studies have shown that under these conditions beryllium mostly demonstrates properties of acceptor impurity, effectively compensating the donor defects in the crystal. It was also found that Be has high mobility in AlN (diffusion constant $D = 10^{-7}$–$10^{-6}\,\mathrm{cm^2/s}$), thanks to which its introduction helps to considerably reduce the optical absorption both in the visible and ultraviolet ranges. We managed to obtain the specimens of Be-doped AlN with the level of optical absorption $\alpha < 30\,\mathrm{cm^{-1}}$ in the spectral area 240–700 nm, which corresponds to best achievements in the area of growth of volume plates of single-crystal AlN.

Funding

This study was conducted under the state assignment FFUG-2024-0024 „Functional materials for microelectronics and photonics“.

Conflict of interest

The authors declare that they have no conflict of interest.

References

[1] J.J.Y. Tsao, S. Chowdhury, M.A. Hollis, D. Jena, N.M. Johnson, K.A. Jones, R.J. Kaplar, S. Rajan, C.G. Van de Walle, E. Bellotti, C.L. Chua, R. Collazo, M.E. Coltrin, J.A. Cooper, K.R. Evans, S. Graham, T.A. Grotjohn, E.R. Heller, M. Higashiwaki, M.S. Islam, P.W. Juodawlkis, M.A. Khan, A.D. Koehler, J.H. Leach, U.K. Mishra, R.J. Nemanich, R.C.N. Pilawa-Podgurski, J.B. Shealy, Z. Sitar, M.J. Tadjer, A.F. Witulski, M. Wraback, J.A. Simmons. Adv. Electron. Mater. **4**, *1*, 1600501 (2018).

[2] C. Zhou, A. Ghods, V.G. Saravade, P.V. Patel, K.L. Yunghans, C. Ferguson, Y. Feng, B. Kucukgok, N. Lu, I.T. Ferguson. ECS J. Solid State Sci. Technol. **6**, *12*, Q149 (2017).

[3] T.Yu. Chemekova, O.V. Avdeev, I.S. Barash, E.N. Mokhov, S.S. Nagalyuk, A.D. Roenkov, A.S. Segal, Yu.N. Makarov, M.G. Ramm, S. Davis, G. Huminic, H. Helava. Physica Status Solidi (c) **5**, *6*, 1612 (2008).

[4] HexaTech press release. HexaTech Demonstrates 2-Inch Aluminum Nitride Substrate with Absorption of 12 cm^{-1} at 265 nm, https://www.hexatechinc.com/news-events.html#jan192021, January 19 (2021).
[5] Crystal IS manufacturing press release. Crystal IS and Asahi Kasei have achieved 99 % usable area on 100 mm bulk aluminum nitride substrate, https://www.cisuvc.com/crystal-is-improves-100 mm-substrate/ (2023).
[6] C. Hartmann, M.P. Kabukcuoglu, C. Richter, A. Klump, D. Schulz, U. Juda, M. Bickermann, D. Hänschke, T. Schröder, T. Straubinger. Appl. Phys. Express **16**, 075502 (2023).
[7] H. Amano, M. Kito, K. Hiramatsu, I. Akasaki. Jpn. J. Appl. Phys. **28**, *12A*, L2112 (1989).
[8] S. Nakamura, T. Mukai, M. Senoh, N. Iwasa. Jpn. J. Appl. Phys. **31**, *2B*, L139 (1992).
[9] M.L. Nakarmi, K.H. Kim, M. Khizar, Z.Y. Fan, J.Y. Lin, H.X. Jiang. Appl. Phys. Lett. **86**, *9*, 092108 (2005).
[10] M.L. Nakarmi, N. Nepal, C. Ugolini, T.M. Altahtamouni, J.Y. Lin, H.X. Jiang. Appl. Phys. Lett. **89**, *15*, 152120 (2006).
[11] H. Ahmad, J. Lindemuth, Z. Engel, C.M. Matthews, T.M. McCrone, W.A. Doolittle. Adv. Mater. **33**, *42*, 2104497 (2021).
[12] V.A. Soltamov, M.K. Rabchinskii, B.V. Yavkin, O.P. Kazarova, S.S. Nagalyuk, V.Yu. Davydov, A.N. Smirnov, V.F. Lebedev, E.N. Mokhov, S.B. Orlinskii, P.G. Baranov. Appl. Phys. Lett. **113**, *8*, 082104 (2018).
[13] N. Nepal, M.L. Nakarmi, H.U. Jang, J.Y. Lin, H.X. Jiang. Appl. Phys. Lett. **89**, *19*, 192111 (2006).
[14] H. Ahmad, Z. Engel, C.M. Matthews, S. Lee, W.A. Doolittle. J. Appl. Phys. **131**, *17*, 175701 (2022).
[15] J.L. Lyons, A. Janotti, C.G. Van de Walle. Jpn. J. Appl. Phys. **52**, *8S*, 08JJ04 (2013).
[16] X. Cai, J. Yang, P. Zhang, S.-H. Wie. Phys. Rev. Appl. **11**, *3*, 034019 (2019).
[17] D.O. Demchenko, M. Vorobiov, O. Andrieiev, T.H. Myers, M.A. Reshchikov. Phys. Rev. Lett. **126**, *2*, 027401 (2021).
[18] O.P. Kazarova, S.S. Nagalyuk, V.A. Soltamov, M.V. Muzafarova, E.N. Mokhov. Semiconductors **56**, *3*, 197 (2022).
[19] E.N. Mokhov, M.K. Rabchinskiy, S.S. Nagalyuk, M.R. Gafurov, O.P. Kazarova. Semiconductors **54**, *3*, 278 (2020).
[20] J.E. Sansonetti, W.C. Martin. J. Phys. Chem. Ref. Data **34**, *4*, 1559 (2005).
[21] A.F.W. Willoughby. Reps. Progr. Phys. **41**, *10*, 1665 (1978).
[22] V.Y. Davydov, Y.E. Kitaev, I.N. Goncharuk, A.N. Smirnov, J. Graul, O. Semchinova, D. Uffmann, M.B. Smirnov, A.P. Mirgorodsky, R.A. Evarestov. Phys. Rev. B **58**, *19*, 12899 (1998).
[23] A. Sarua, M. Kuball, J.E. Van Nostrand. Appl. Phys. Lett. **81**, *8*, 1426 (2002).
[24] M. Kuball, J.M. Hayes, Y. Shi, J.H. Edgar. Appl. Phys. Lett. **77**, *13*, 1958 (2000).
[25] V.A. Soltamov, I.V. Ilyin, A.A. Soltamova, D.O. Tolmachev, E.N. Mokhov, P.G. Baranov. Diamond. Relat. Mater. **20**, *7*, 1085 (2011).
[26] V.A. Soltamov, I.V. Ilyin, A.A. Soltamova, D.O. Tolmachev, N.G. Romanov, A.S. Gurin, E.N. Mokhov, P.G. Baranov. Physica Status Solidi (c) **9**, *3–4*, 745 (2012).
[27] Q. Yan, A. Janotti, M. Scheffler, C.G. Van de Walle. Appl. Phys. Lett. **105**, *11*, 111104 (2014).
[28] R. Collazo, J. Xie, B.E. Gaddy, Z. Bryan, R. Kirste, M. Hoffmann, R. Dalmau, B. Moody, Y. Kumagai, T. Nagashima, Y. Kubota, T. Kinoshita, A. Koukitu, D.L. Irving, Z. Sitar. Appl. Phys. Lett. **100**, *19*, 191914 (2012).
[29] K. Irmscher, C. Hartmann, C. Guguschev, M. Pietsch, J. Wollweber, M. Bickermann. J. Appl. Phys. **114**, *12*, 123505 (2013).
[30] V.A. Soltamov, I.V. Ilyin, A.A. Soltamova, D.O. Tolmachev, E.N. Mokhov, P.G. Baranov. Phys. Solid State **53**, *6*, 1186 (2011).
[31] X.T. Trinh, D. Nilsson, I.G. Ivanov, E. Janzén, A. Kakanakova-Georgieva, N.T. Son. Appl. Phys. Lett. **105**, *16*, 162106 (2014).

Translated by M.Verenikina